Na^+-activated K^+ channels localized in the nodal region of myelinated axons of *Xenopus*

Duk-Su Koh*, Peter Jonas* and Werner Vogel

*Physiologisches Institut, Justus-Liebig-Universität, Aulweg 129, D-35392 Giessen, Germany and *Max-Planck-Institut für medizinische Forschung, Abteilung Zellphysiologie, Jahnstrasse 29, D-69120 Heidelberg, Germany*

1. A potassium channel activated by internal Na^+ ions (K^+_{Na} channel) was identified in peripheral myelinated axons of *Xenopus laevis* using the cell-attached and excised configurations of the patch clamp technique.

2. The single-channel conductance for the main open state was 88 pS with $[K^+]_o = 105$ mM and 34 pS with $[K^+]_o = 2{\cdot}5$ mM ($[K^+]_i = 105$ mM). The channel was selectively permeable to K^+ over Na^+ ions. A characteristic feature of the K^+_{Na} channel was the frequent occurrence of subconductance states.

3. The open probability of the channel was strongly dependent on the concentration of Na^+ ions at the inner side of the membrane. The half-maximal activating Na^+ concentration and the Hill coefficient were 33 mM and 2·9, respectively. The open probability of the channel showed only weak potential dependence.

4. The K^+_{Na} channel was relatively insensitive to external tetraethylammonium (TEA^+) in comparison with voltage-dependent axonal K^+ channels; the half-maximal inhibitory concentration (IC_{50}) was 21·3 mM (at −90 mV). In contrast, the channel was blocked by low concentrations of external Ba^{2+} and Cs^+ ions, with IC_{50} values of 0·7 and 1·1 mM, respectively (at −90 mV). The block by Ba^{2+} and Cs^+ was more pronounced at negative than at positive membrane potentials.

5. A comparison of the number of K^+_{Na} channels in nodal and paranodal patches from the same axon revealed that the channel density was about 10-fold higher at the node of Ranvier than at the paranode. Moreover, a correlation between the number of K^+_{Na} channels and voltage-dependent Na^+ channels in the same patches was found, suggesting co-localization of both channel types.

6. As weakly potential-dependent ('leakage') channels, axonal K^+_{Na} channels may be involved in setting the resting potential of vertebrate axons. Simulations of Na^+ ion diffusion suggest two possible mechanisms of activation of K^+_{Na} channels: the local increase of Na^+ concentration in a cluster of Na^+ channels during a single action potential or the accumulation in the intracellular axonal compartment during a train of action potentials.

A potassium channel activated by internal sodium ions (designated as the K^+_{Na} channel) was first described in mammalian cardiac cells (Kameyama, Kakei, Sato, Shibasaki, Matsuda & Irisawa, 1984) and later in the somata of neurones (Bader, Bernheim & Bertrand, 1985; Dryer, Fujii & Martin, 1989). In heart myocytes, the channel was suggested to be activated under pathophysiological conditions, for instance, during failure of the Na^+–K^+ pump (Kameyama *et al.* 1984). In neuronal cell bodies, it was proposed that K^+_{Na} channels could be involved in setting the resting potential (Dryer *et al.* 1989; Haimann, Bernheim, Bertrand & Bader, 1990). Measurements on excised membrane patches, however, demonstrated that K^+_{Na} channels require relatively high Na^+ concentrations (above 10–20 mM) to be activated (Kameyama *et al.* 1984; Dryer *et al.* 1989; Haimann *et al.* 1990; Egan, Dagan, Kupper & Levitan, 1992). Since estimates of the internal Na^+ concentration in somata of neurones range widely, from 5 to 50 mM (Bührle & Sonnhof, 1983; Galvan, Dörge, Beck & Rick, 1984), it remains unclear if the channels are active in resting cells. Moreover, it was suggested that K^+_{Na} channels could be triggered by the Na^+ entry during a single action potential (Bader *et al.* 1985) and therefore might be involved in spike

repolarization. However, it has been questioned on theoretical grounds whether the influx of Na^+ ions through a voltage-dependent Na^+ channel would be sufficient to activate a K^+_{Na} channel even if both were co-localized microscopically (Dryer, 1991).

One would expect that the conditions for the activation of the K^+_{Na} channel might be more favourable in small processes of neurones, like axons and dendrites, than in the somata of nerve cells. At the node of Ranvier of myelinated axons, Na^+ channels are concentrated at an extremely high density around a very small intracellular volume, suggesting accumulation of Na^+ ions in the nodal compartment after trains of action potentials. The data of Bergman (1970), in fact, supported the idea that a considerable increase of internal Na^+ concentration occurs during repetitive stimulation in myelinated nerve fibres. However, there was no direct evidence that K^+_{Na} channels might be present in the axonal membrane. It was noted that post-tetanic after-hyperpolarizations in myelinated nerve depended on internal Na^+ but were not due to activity of electrogenic pumps (Hurlbut, 1965), leading Stämpfli & Hille (1976) to conclude that 'some link is missing to explain all these observations'.

A systematic investigation of the effects of internal Na^+ concentration on axonal ionic channels, however, was not possible until the patch clamp technique could be applied to nerve fibres which were demyelinated *in vitro* (Jonas, Bräu, Hermsteiner & Vogel, 1989). This method allows high-resolution current recording as well as free access to the intracellular side of the axonal membrane (Jonas, Koh, Kampe, Hermsteiner & Vogel, 1991). Using this technique, we identified an axonal K^+ channel which is activated by internal Na^+ ions. With respect to conductance, gating and pharmacological properties, the channel showed many similarities with K^+_{Na} channels in the heart and somata of neurones described previously. It seemed particularly interesting to address the question of co-localization between K^+_{Na} channels and voltage-dependent Na^+ channels in axons, because the node of Ranvier is characterized by a uniquely steep gradient of Na^+ channel density (see Hille, 1992). As a prerequisite for such an analysis, it was necessary to identify the nodal region in demyelinated axons. Some of these results have been reported in abstract form (Koh & Vogel, 1992).

METHODS

Preparation and patch clamp technique

Amphibian nerve fibres were enzymatically demyelinated as described previously to make the axolemma accessible for patch pipettes (Jonas *et al.* 1989, 1991). Briefly, adult clawed toads (*Xenopus laevis*) were decapitated and the tibial and peroneal nerves were dissected. The nerve trunks were desheathed and incubated in Ringer solution containing 3·5 mg ml^{-1} of collagenase (Worthington type CLS II, Biochrom, Berlin, Germany) for 135 min to digest the endoneural collagen fibres. Subsequently, they were treated with 1 mg ml^{-1} of protease (Type XXIV, Sigma, St Louis, MO, USA) in Ca^{2+}-free Ringer solution for 35 min to break up the axoglial junctions adjacent to the nodes of Ranvier. During the incubation, temperature was kept constant at $23·5 \pm 0·3$ °C and mild shaking was applied to facilitate the access of the enzymes to all parts of the nerve. After incubation, the nerve was cut into segments (about 3–4 mm in length). The fibres were dissociated by gentle stirring and were then transferred into plastic cell culture dishes, the bases of which had been coated with a thin layer of laboratory grease (Glisseal Blue, Borer Chemie, Solothurn, Switzerland). Experiments were done on fibres with a myelin sheath diameter of >10 μm.

Patch clamp recordings were obtained as described previously (Hamill, Marty, Neher, Sakmann & Sigworth, 1981). The patch pipettes were pulled from borosilicate glass tubing (GC150, Clark Electromedical Instruments, Pangbourne, UK), and heat polished before use. In many experiments, they were coated with Sylgard 184 (Dow Corning, Seneffe, Belgium). When filled with internal solution, the pipettes had a resistance of 5–20 MΩ. Membrane current was measured using an EPC-7 patch clamp amplifier (List, Darmstadt, Germany), filtered with its internal 10 kHz filter, and stored on videotape via a modified PCM-501ES pulse code modulation unit (Sony, Tokyo, Japan). For analysis, data were replayed from tape, filtered with a 4-pole low-pass Bessel filter, and re-digitized with a Labmaster TM-40 AD/DA board (Scientific Solutions, Solon, OH, USA) attached to a personal computer. The corner frequency of the low-pass filter (−3 dB) and the sampling frequency were 1 and 4 kHz, respectively. In the experiments where K^+_{Na} and voltage-dependent Na^+ channels were recorded in the same membrane patch (Fig. 8), voltage pulses were generated via the DA unit of the Labmaster board. Simultaneously, the current was digitized by the AD unit and stored on-line using commercially available software (pCLAMP, Axon Instruments, Foster City, CA, USA). In these experiments, the filter and the sampling frequencies were 3 and 20 kHz, respectively. All recordings were made at 13 ± 1 °C. Electrophysiological data were obtained from 104 membrane patches in total (axon-attached, inside-out and outside-out configurations). Although in outside-out patches changes of the internal Na^+ concentration (100 mM) could not be readily made, K^+_{Na} channels could be unequivocally distinguished from other axonal channels on the basis of high unitary conductance, weak voltage dependence and the presence of multiple subconductance states.

Solutions

The Ringer solution contained (mM): 110 NaCl, 2·5 KCl, 2 $CaCl_2$ and 3 *N*-(2-hydroxyethyl)piperazine-*N'*-(2-ethanesulphonic acid) (Hepes), pH adjusted to 7·4 with NaOH. The 2·5 mM K^+_o external solution in addition contained 100 mM choline chloride. The 105 mM K^+_o external solution contained (mM): 105 KCl, 13 NaCl, 2 $CaCl_2$, 100 choline chloride and 3 Hepes, pH adjusted to 7·4 with KOH. In most of the measurements (except the experiments where voltage-activated Na^+ channels were recorded, see Fig. 8), 100 nM tetrodotoxin (TTX) was added to the external solutions.

The 105 mM K^+_i (internal solution) contained (mM): 105 KCl, 100 NaCl, 3 Hepes, 3 ethyleneglycol-bis-[β-aminoethylether]-*N,N,N',N'*-tetraacetic acid (EGTA), pH adjusted to 7·4 with KOH. In the experiments where the open probability of the K^+_{Na} channel was measured as a function of the internal

concentration of Na^+ ions, the Na^+ concentration was reduced and choline chloride was added accordingly to maintain osmolarity. Tetraethylammonium chloride (TEA-Cl) and $BaCl_2$ were from Merck (Darmstadt, Germany); CsCl was from Sigma. For solution exchange on excised membrane patches, a multi-barrel perfusion system was used (Yellen, 1982).

Lucifer Yellow staining and immunohistochemistry

For intracellular staining of axons with Lucifer Yellow (LY), patch pipettes were filled with an internal solution containing 1% LY CH (dilithium salt, Sigma; the solution was passed through 0·2 μm pore size filters before use). Five to ten minutes after forming the seal and breaking the patch membrane, the nerve fibre was inspected using epifluorescence optics. In all sixty trials, the axon was stained in both directions and over long distances, sometimes over several nodes of Ranvier. The nodal region was inspected at high magnification using an Axiovert 135 microscope (Zeiss, Oberkochen, Germany) and a ×63 oil immersion objective lens (numerical aperture 1·4).

For immunohistochemical staining, nerve fibres were incubated for 1 h with polyclonal anti-galactocerebroside antibodies from rabbit (Chemicon, London, UK; diluted 1:20 in Ringer solution), a specific marker of myelin membrane (see Ranscht, Clapshaw, Price, Noble & Seifert, 1982). Then the fibres were washed four times with a large volume of Ringer solution and incubated for 1 h with a fluorescein isothiocyanate-conjugated anti-rabbit IgG from goat (Chemicon; diluted 1:20 in Ringer solution, passed through 0·2 μm filters to eliminate precipitate). The whole procedure was done at room temperature. After washing four times with Ringer solution, the fibres were inspected using epifluorescence optics.

Analysis

It has been reported that K^+_{Na} channels show subconductance states (Haimann *et al.* 1990; Wang, Kimitsuki & Noma, 1991; Dryer, 1993) and run-down of channel activity (Egan *et al.* 1992; Dryer, 1993), which might complicate the quantitative analysis of both conductance and gating properties. Axonal K^+_{Na} channels showed subconductance states at various current levels (Figs 2 and 5). The single-channel current corresponding to the main conductance state was therefore measured from sections of recording of length 250–640 ms on a computer screen using cursors. Rundown of channel activity in excised patches, which was reported for K^+_{Na} channel subtypes in olfactory bulb neurones (Egan *et al.* 1992; Dryer, 1993), was not apparent for axonal K^+_{Na} channels. The apparent open probability of the channel (P_{open}) was thus obtained from 12 to 32 s sections of recording using the equation: $P_{open} = I/(iN)$, where I is the mean current during the recording period, i is the single-channel current of the main conductance state, and N is the number of K^+_{Na} channels present in the patch. N was estimated from the maximum number of superimposed K^+_{Na} channel events observed during long recordings (> 1 min) with 100 mM Na^+ on the inner side of the membrane. Using this definition, a channel dwelling in a subconductance state with, for example, 10% current amplitude of the main conductance value and a channel which is fully open for only 10% of the time would give the same contribution to P_{open}. P_{open} calculated in this way should thus predict the macroscopic current mediated by several K^+_{Na} channels.

The amplitudes of the subconductance levels were analysed using the variance–mean method described by Patlak (1988). A window with a width of five points (corresponding to 1 ms) was shifted over the discretely sampled data record. The mean and variance of the data points within each window were calculated. A 'levels histogram' (Patlak, 1988; see Fig. 5*B*) was constructed, including mean values only if the corresponding variances were below a specified threshold (σ_{crit}^2). σ_{crit} was set to 0·12 pA, a value comparable to the standard deviation of the background noise (0·18 pA in the experiment shown in Fig. 5). A non-linear least-squares fit was performed using a modified Gauss–Newton algorithm. Numerical values are given as means ± standard error of the mean (S.E.M.). Error bars in the figures also indicate S.E.M.; they were plotted only when they exceeded the size of symbols.

Simulation of diffusion of Na^+ ions

The three-dimensional diffusion of Na^+ ions from the inner mouth of a voltage-dependent Na^+ channel can be described by equations for radial diffusion from a point source representing the channel mouth into a semi-infinite medium as follows (Crank, 1975, p. 29; Dryer, 1991):

$$dc = \Phi_{channel}\, dt/[4(\pi Dt)^{3/2}]\exp[-r^2/(4Dt)], \quad (1)$$

where c is the concentration of Na^+ ions, D is the diffusion coefficient, $\Phi_{channel}$ is the Na^+ influx through a single Na^+ channel, t is time (assuming that the channel opens at $t = 0$), and r is the radial distance from the channel mouth. Integration of eqn (1) with respect to time yields:

$$c = \Phi_{channel}/(2\pi Dr)\mathrm{erfc}[r/(4Dt)^{1/2}], \quad (2)$$

where erfc is the error function complement. The concentration of Na^+ ions at the centre of a hexagonal array of Na^+ channels was calculated by adding the increases of $[Na^+]_i$ arising from all individual point sources.

The accumulation of Na^+ ions in the axonal compartment during a train of action potentials was simulated assuming one-dimensional diffusion from a plane source representing the nodal compartment to both sides of a cylinder with infinite length and unit cross-section as follows (Crank, 1975, p. 11):

$$dc = \Phi_{train}\, dt/[2(\pi Dt)^{1/2}]\exp[-x^2/(4Dt)], \quad (3)$$

where Φ_{train} is the Na^+ influx during a train of spikes, t is time (assuming that the train of spikes starts at $t = 0$), and x is the distance from the plane of Na^+ influx. Integration of eqn (3) with respect to time yields:

$$c = \Phi_{train}\, x/(4\pi^{1/2}D)\Gamma[-\tfrac{1}{2}, x^2/(4Dt)], \quad (4)$$

where Γ is the incomplete gamma function. Diffusion equations were solved and plotted using Mathematica (Version 2·1, Wolfram Research, Champaign, IL, USA) running on a Macintosh computer.

The amount of Na^+ influx through a single open Na^+ channel was assumed to be $\Phi_{channel} = 1{\cdot}04 \times 10^{-17}$ M s^{-1}, corresponding to 1 pA. The Na^+ influx during a single action potential was estimated from the integral under the $I_{Na}(t)$ curve using models of nodal excitability as described previously (Frankenhaeuser & Huxley, 1964). For a $[Na^+]_i$ of 13·7 mM, it was calculated as $1{\cdot}4 \times 10^{-17}$ M for an axon with a radius of 5 μm and a nodal gap width of 1 μm. The amount of Na^+ influx during a train of action potentials (250 s^{-1}) can then be obtained as $\Phi_{train} = 3{\cdot}5 \times 10^{-15}$ M s^{-1}. When $[Na^+]_i$ was

doubled, the corresponding value of Φ_{train} decreased by only 12%; Φ_{train} was therefore assumed to be constant to keep the calculations as simple as possible. The activity of the Na^+–K^+ pump was neglected.

RESULTS

Location of the nodal region in enzymatically demyelinated axons

Previous electron microscopic studies on the structure of intact myelinated nerve fibres demonstrated that the paranodal end segments of the axon are constricted, to about one-half of the internodal diameter (Berthold & Rydmark, 1983). The nodal axon segment located in the centre of this constriction shows a slight barrel-shaped increase in diameter ('central bulge': Berthold, 1978; Berthold & Rydmark, 1983). Some of the demyelinated axons, in the high-power light microscopic view as well as under epifluorescence optics, after they were filled with Lucifer Yellow, showed a similar structure (Fig. 1*A* and *B*). Immunohistochemical staining using a specific Schwann cell marker, an antibody against galactocerebroside, excluded the possibility that the axon in this region might still be covered by fragments of Schwann cell membrane (Fig. 1*C* and *D*). It therefore seemed likely that some demyelinated axons retained the structural elements present in intact fibres, and that the central bulge corresponded to the exact location of the previous node of Ranvier. Further evidence for this assumption was obtained by studying microscopically the demyelination process as a function of time. When a myelinated nerve fibre, after enzymatic treatments, attached to the grease-coated base of the dish (see Methods), the myelin sheath retracted to both sides of the node of Ranvier, and the axonal constriction became visible. When a central bulge was apparent, its location was always identical to the site of the previous node (data not shown). Finally, the density of voltage-dependent Na^+ channels was roughly 100-fold higher in membrane patches from the central bulge than in paranodal patches, with peak inward currents up to 200 pA (measured in external Ringer solution, −30 mV, 20 MΩ pipette resistance). In the following, we therefore denote this part of the demyelinated axon as the 'nodal region'.

Electrophysiological properties of the axonal K^+_{Na} channel

In more than 50% of all membrane patches isolated from the nodal region of demyelinated axons, a large-conductance channel was observed when the internal Na^+ concentration was above 20 mM. Figure 2*A* and *B* shows single-channel events with 105 and 2·5 mM K^+_o on the outer side of the membrane, respectively; the internal solution was 105 mM K^+_i containing 100 mM Na^+ ions. A characteristic property of the channel was the frequent

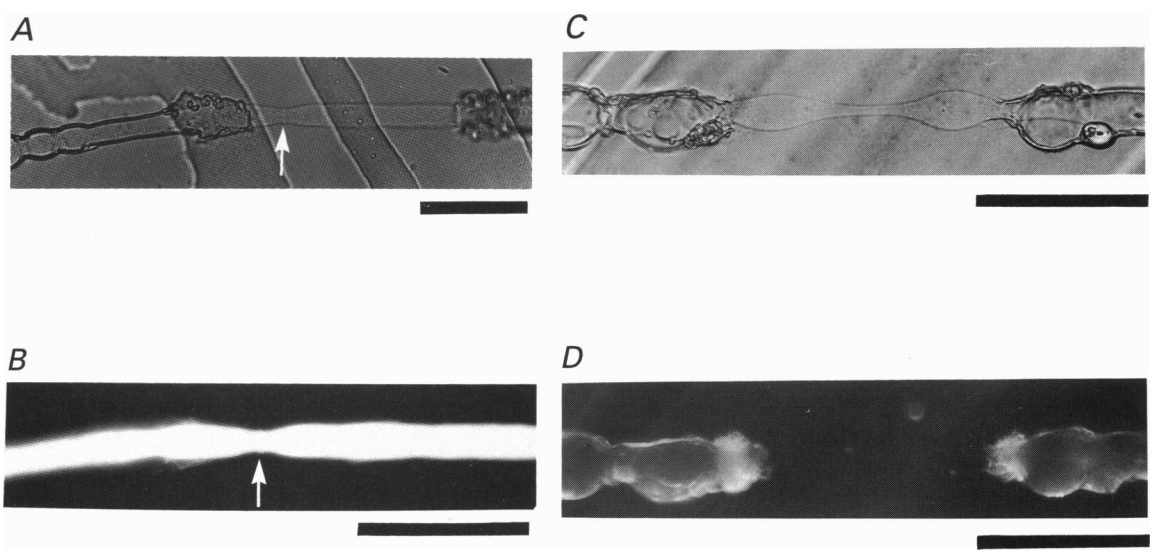

Figure 1. Morphology of enzymatically demyelinated axons
A and *B*, a demyelinated axon filled with Lucifer Yellow, under Nomarski differential interference contrast optics (*A*) and epifluorescence optics (*B*). The axon is spanned between the retracted myelin sheaths on either side. Note the constricted axon segment and the protrusion of the axolemma in the very centre (arrows). This region most probably corresponds to the previous node of Ranvier. *C* and *D*, view of a nerve fibre stained immunohistochemically using antibodies against galactocerebroside; light microscopy (*C*), and epifluorescence optics (*D*). For both staining procedures, dishes with bases made from glass coverslips were used. The base of the dish was coated with a thin layer of Glisseal Red rather than Glisseal Blue, because the former showed a lower level of autofluorescence. Scale bars 50 μm. For further details see Methods.

occurrence of subconductance states to various levels in both 105 and 2·5 mM K_o^+ solutions and at all membrane potentials (E_m). Current–voltage (i–E_m) relations for the main conductance level obtained from several patches are illustrated in Fig. 2*C*. With 105 mM K_o^+, the single-channel current reversed close to 0 mV. The i–E_m relation was almost linear; a slight reduction of the conductance at very negative and positive potentials was observed. Linear regression of the data points between −60 and 40 mV revealed an elementary conductance of 88 pS. In 2·5 mM K_o^+ solution, the reversal potential shifted to negative values, whereas the shape of the i–E_m relation remained almost linear. Fitting the data points between −70 and 40 mV with a straight line yielded an extrapolated reversal potential of −74·8 mV and a single-channel conductance of 34 pS. From the reversal

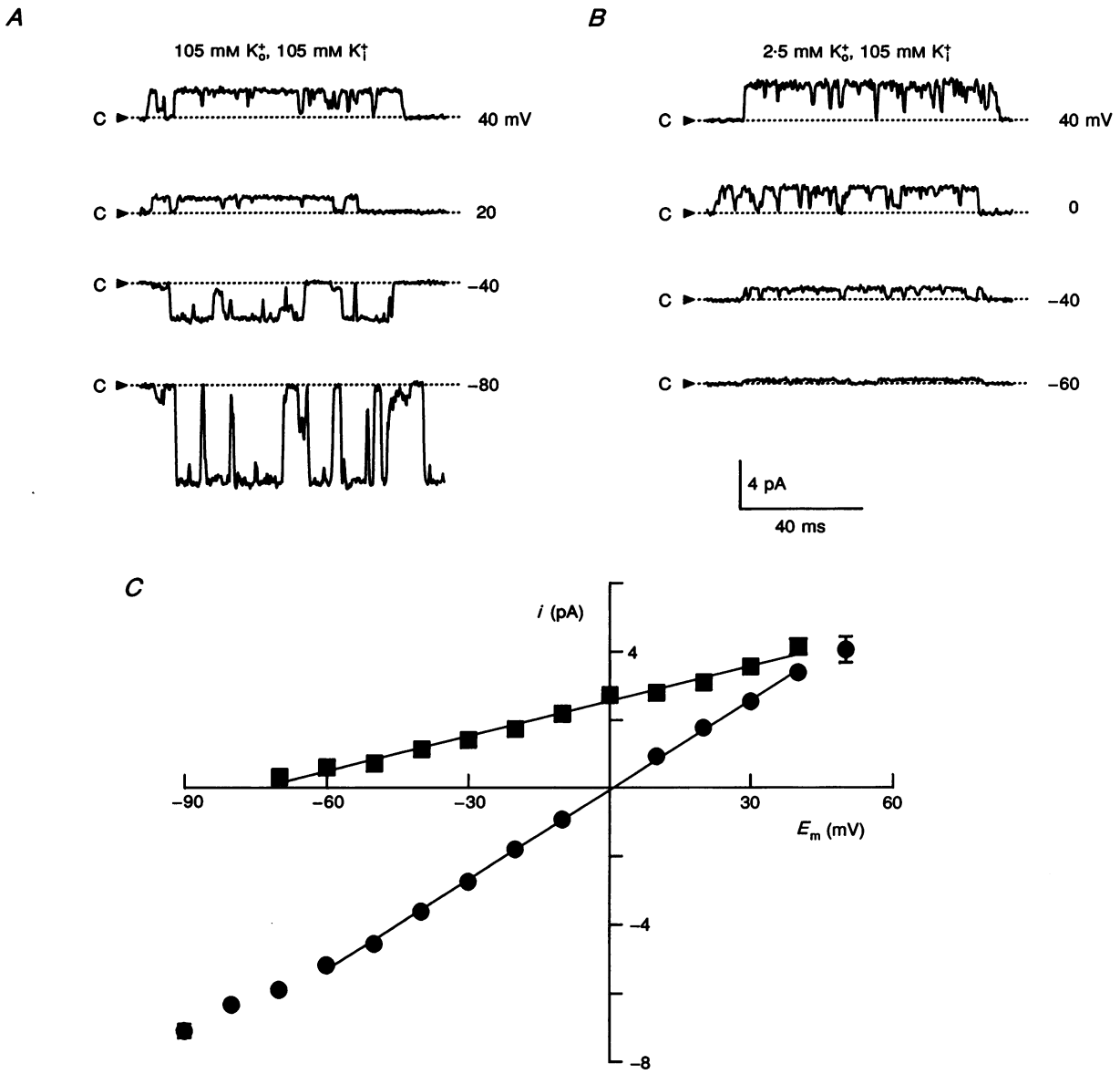

Figure 2. Single-channel conductance of axonal K^+_{Na} channels
A and *B*, recordings of single-channel events obtained from an outside-out patch at different membrane potentials as indicated. Bath: 105 mM (*A*) and 2·5 mM K_o^+ solution (*B*); pipette: 105 mM K_i^+ containing 100 mM Na^+. Note the subconductance levels. Current level when the channels are closed (C) is marked by an arrowhead. *C*, single-channel current (i) of the main conductance state plotted against membrane potential (E_m) with 105 mM K_o^+, 105 mM K_i^+ solutions (●, data from 1 inside-out and 5 outside-out patches) and with 2·5 mM K_o^+, 105 mM K_i^+ solution (■, data from 3 outside-out patches). Data points within a given range of membrane potentials (−60 to 40 mV and −70 to 40 mV, respectively) were fitted using linear regression, revealing conductances of 88 pS in 105 mM K_o^+ and 34 pS in 2·5 mM K_o^+.

potential, the relative permeability of the channel to Na^+ ions as compared to K^+ ions could be calculated as $P_{Na}/P_K = 0{\cdot}035$ using the Goldman–Hodgkin–Katz voltage equation (Hille, 1992). This indicates that the channel is selectively permeable to K^+ ions. Extrapolated reversal potential and P_{Na}/P_K values given above represent upper limits if the i–E_m relation was curved concavely, a tendency which is predicted by the Goldman–Hodgkin–Katz current equation (Hille, 1992).

The dependence of channel activity on the internal Na^+ concentration ($[Na^+]_i$) was characterized at a membrane potential of −90 mV using inside-out patches. Figure 3*A* shows representative recordings from a patch to which internal Na^+ concentrations of 2, 20 and 50 mM were applied subsequently. With 2 mM $[Na^+]_i$, almost no channel openings were observed. With higher $[Na^+]_i$ (20 and 50 mM), the activity of the channel increased in a concentration-dependent manner. Figure 3*B* shows a plot of the apparent open probability (calculated as described in Methods, data from 3 patches) against $[Na^+]_i$. A non-linear fit of the data points with the Hill equation yielded a half-maximal activating concentration of 32·5 mM and a Hill coefficient of 2·85, suggesting that the channel had at least three internal binding sites for Na^+ ions. The maximal open probability was 0·45, i.e. considerably lower than 1. This was due to the fact that even at high $[Na^+]_i$

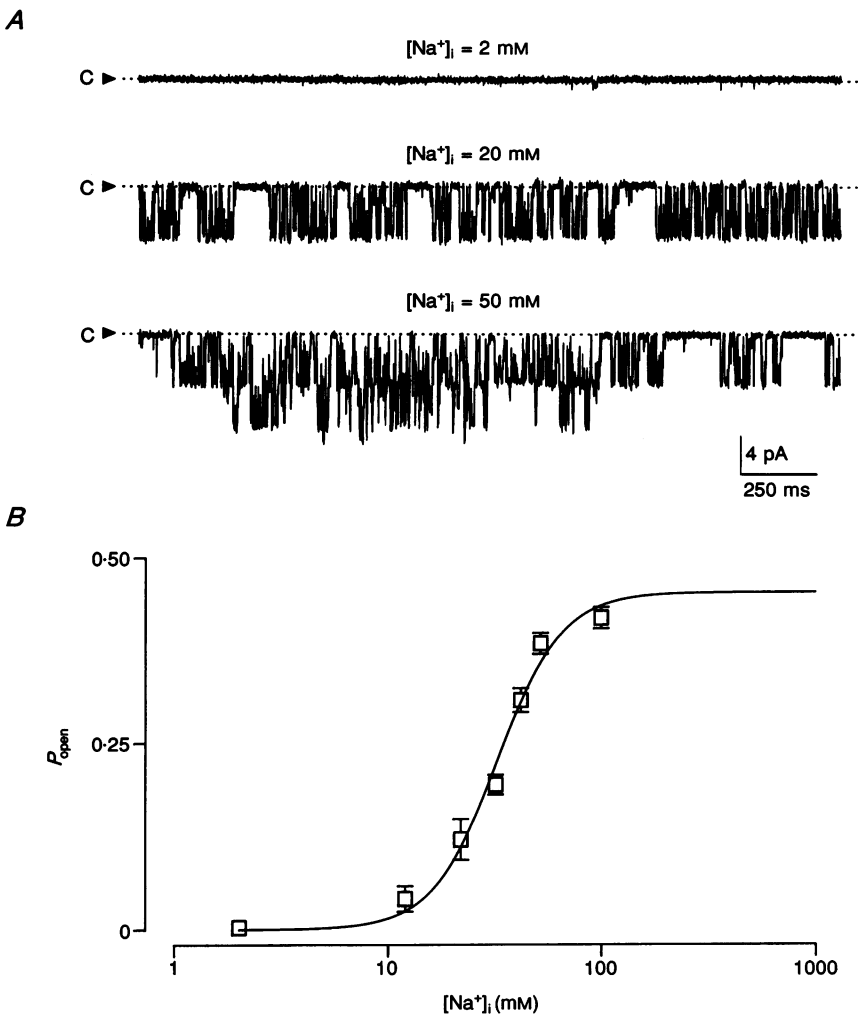

Figure 3. Activation of axonal K^+_{Na} channels by internal Na^+ ions
A, recordings of single-channel events from an inside-out patch. Bath: 105 mM K^+_i containing different concentrations of Na^+ ions; pipette: 105 mM K^+_o. Membrane potential −90 mV. The patch contained two K^+_{Na} channels. *B*, open probability (P_{open}) plotted against concentration of Na^+ ions at the inner side of the membrane ($[Na^+]_i$). P_{open} was calculated as described in Methods. Data were from three inside-out patches. Same experimental conditions as in *A*. The curve was drawn according to the equation $f([Na^+]_i) = P_{open,max}\,[1 + (K_D/[Na^+]_i)^{n_H}]^{-1}$, with dissociation constant (K_D) = 32·5 mM, Hill coefficient (n_H) = 2·85 and maximal open probability ($P_{open,max}$) = 0·45 as obtained by non-linear least-squares fit.

concentrations the channel dwelled in the closed state and, additionally, in the subconductance states for a considerable fraction of time.

The dependence of channel activity on the membrane potential was studied under stationary conditions for a constant $[Na^+]_i$ concentration of 100 mM. Figure 4*A* illustrates typical recordings at 40 and −90 mV, and Fig. 4*B* shows a plot of the apparent P_{open} against membrane potential. The activity of the channel was only slightly potential dependent, being somewhat higher at positive than at negative voltages: the open probability was 0·59 ± 0·04 at 40 mV and 0·37 ± 0·02 at −90 mV (6 patches). In summary, P_{open} was strongly dependent on $[Na^+]_i$ but only weakly dependent on membrane potential. Together with the linearity of single-channel i–E_m relations, this predicts that at a fixed internal Na^+ concentration the K^+_{Na} channel could appear as a potassium-selective 'leakage' conductance in macroscopic current measurements.

A characteristic feature of the axonal K^+_{Na} channel was the frequent occurrence of subconductance states (see also Haimann *et al.* 1990; Wang *et al.* 1991; Egan *et al.* 1992; Dryer, 1993). The point amplitude histogram derived from a long section of recording with $[Na^+]_i = 100$ mM and a membrane potential of −90 mV suggests the presence of several sublevels between the closed state and the main open state (Fig. 5*A*). To estimate the relative fraction of time the channel spent in these subconductance states, the histogram peaks corresponding to the closed and the main open state were fitted with Gaussian functions. In the experiment shown in Fig. 5 (in which the apparent P_{open} was 0·48; see above and Methods) the probabilities of being in the closed and the main open state were estimated as 0·37 and 0·32, respectively. In the remaining fraction of time (0·31), the channel dwelled in subconductance states or switched between different conductance levels.

The possible presence of subconductance states with discrete amplitudes was investigated using the variance–mean analysis (Patlak, 1988; see Methods). In the 'levels histogram' shown in Fig. 5*B*, at least three discrete subconductance levels could be identified besides the closed and the main open state. The current amplitudes of the substates were roughly integer multiples of 1/10 of the current level in the main open state. Figure 5*C* shows examples of different subconductance levels, and demonstrates furthermore that they were reached from the closed as well as from the main open state.

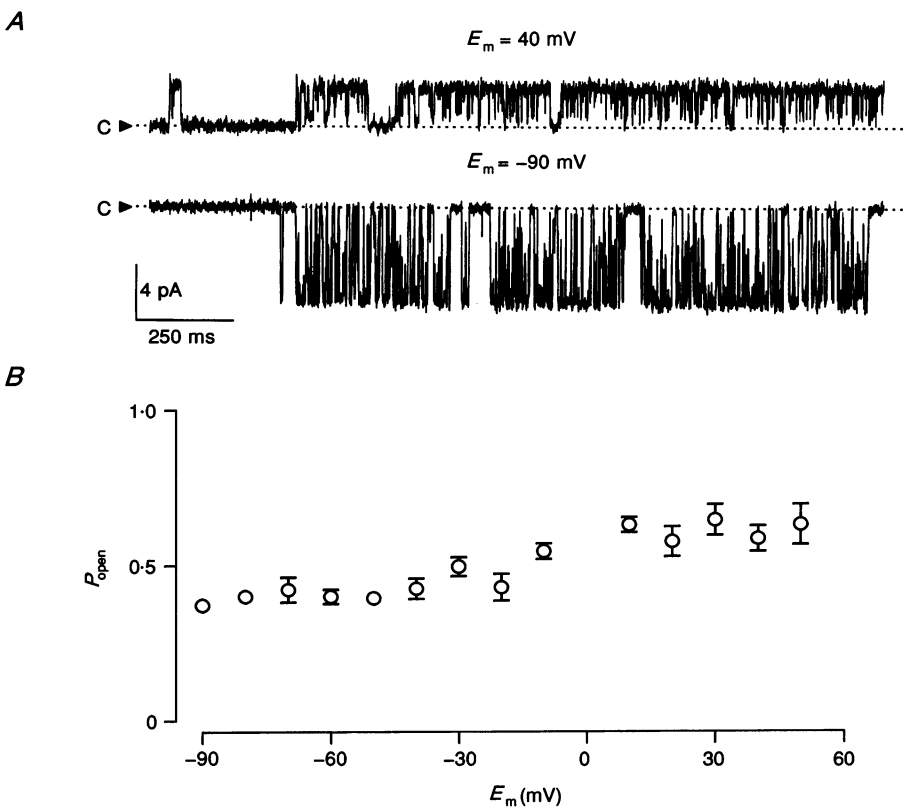

Figure 4. Potential dependence of open probability of axonal K^+_{Na} channels
A, recordings at different membrane potentials (40 and −90 mV) from an outside-out patch containing one K^+_{Na} channel. Bath: 105 mM K^+_o; pipette: 105 mM K^+_i containing 100 mM Na^+. *B*, open probability (P_{open}) plotted against membrane potential. Data were obtained under the same conditions as in *A*; 6 outside-out patches.

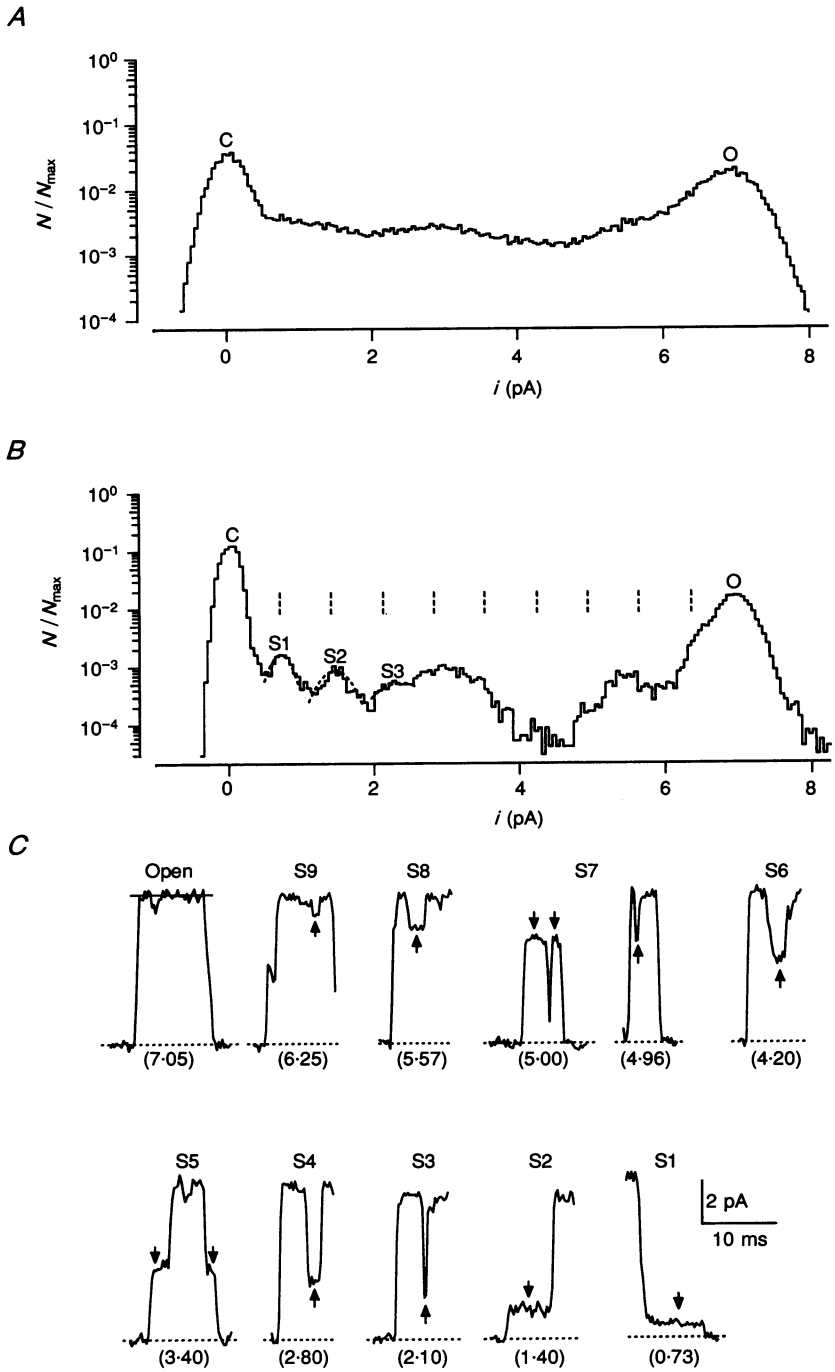

Figure 5. Multiple subconductance states

A, point amplitude histogram derived from a 200 s recording. Inside-out patch. Bath: 105 mM K_i^+ containing 100 mM Na^+; pipette: 105 mM K_o^+; membrane potential −90 mV. *B*, point amplitude histogram from the same recording as in *A* using the variance–mean analysis described in Methods. Current values of the first three subconductance states were obtained by fitting the respective peaks separately with Gaussian functions, yielding mean values of 0·71, 1·46 and 2·37 pA, respectively. Vertical dashed lines indicate integer multiples of 1/10 of the current of the main conductance state (7·05 pA). *C*, examples of different subconductance states from the same recording as in *A* and *B*; current values of each of the subconductance states (denoted by arrows in each trace) are given in parentheses (in pA).

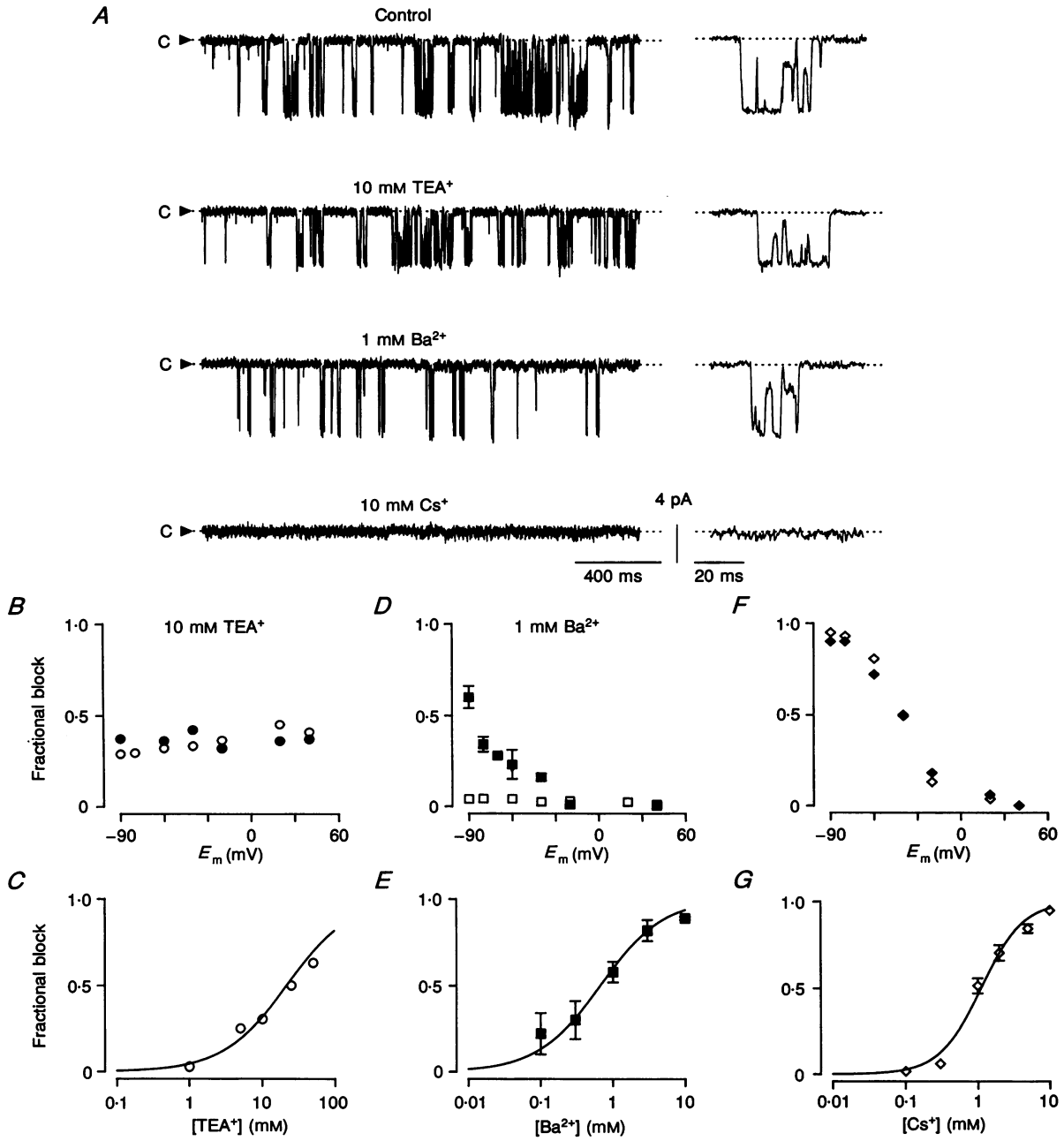

Figure 6. Block of axonal K^+_{Na} channels by external TEA^+, Ba^{2+} and Cs^+ ions
A, unitary currents in 105 mM K^+_o (control) and in 105 mM K^+_o with 10 mM TEA^+, 1 mM Ba^{2+} and 10 mM Cs^+, respectively. Outside-out patch. Pipette: 105 mM K^+_i containing 100 mM Na^+. Membrane potential −90 mV. Recordings on the right are shown on an expanded time scale. *B*, *D* and *F*, fractional block of single-channel current (open symbols) and mean current (filled symbols) by 10 mM TEA^+ (*B*), 1 mM Ba^{2+} (*D*) and 10 mM Cs^+ (*F*), plotted against membrane potential. Data from the same membrane patch as in *A* except *D*, where data from two patches were pooled. *C*, *E* and *G*, fractional block plotted against concentration (c) of TEA^+ (*C*), Ba^{2+} (*E*) and Cs^+ (*G*); block of single-channel current in *C* and *G*, and mean current in *E*. Data from 6, 4 and 4 outside-out patches, respectively; membrane potential −90 mV. Curves represent the function $f(c) = [1 + (IC_{50}/c)^{n_H}]^{-1}$, with half-maximal inhibitory concentrations (IC_{50}) of 21·3, 0·7 and 1·1 mM and Hill coefficients (n_H) of 1·0, 1·0 and 1·48 for TEA^+, Ba^{2+} and Cs^+, respectively, as obtained by non-linear least-squares fit.

Pharmacological properties of the axonal K^+_{Na} channel

To study the pharmacological profile of the axonal K^+_{Na} channel, the effects of the K^+ channel blockers TEA^+, Ba^{2+} and Cs^+ were investigated using outside-out patches. All of them reversibly blocked the channel; however, differences were observed with respect to kinetics of block, voltage dependence and binding affinity. In the presence of 10 mM external TEA^+, the single-channel current at a membrane potential of −90 mV was smaller compared with control conditions (Fig. 6*A*). Single-channel current and mean current during a long recording section were reduced to a similar extent, suggesting that the open probability of K^+_{Na} channels remained unchanged (Fig. 6*B*). The binding and dissociation of TEA^+ thus seemed to occur on a very fast time scale (see Hille, 1992). When the fractional block is plotted against membrane potential, it can be seen that TEA^+ acts in an almost potential-independent way (Fig. 6*B*). In Fig. 6*C*, the fractional block of single-channel current at −90 mV was shown as a function of the TEA^+ concentration. The data points could be satisfactorily described using an adsorption isotherm with a half-maximal inhibitory concentration, IC_{50}, of 21·3 mM. The K^+_{Na} channel is thus relatively TEA^+ insensitive as compared to other axonal K^+ channels (Jonas *et al.* 1989, 1991; Koh, Jonas, Bräu & Vogel, 1992).

In contrast to the block by TEA^+, 1 mM external Ba^{2+} at −90 mV reduced the channel activity without any noticeable effect on the single-channel conductance

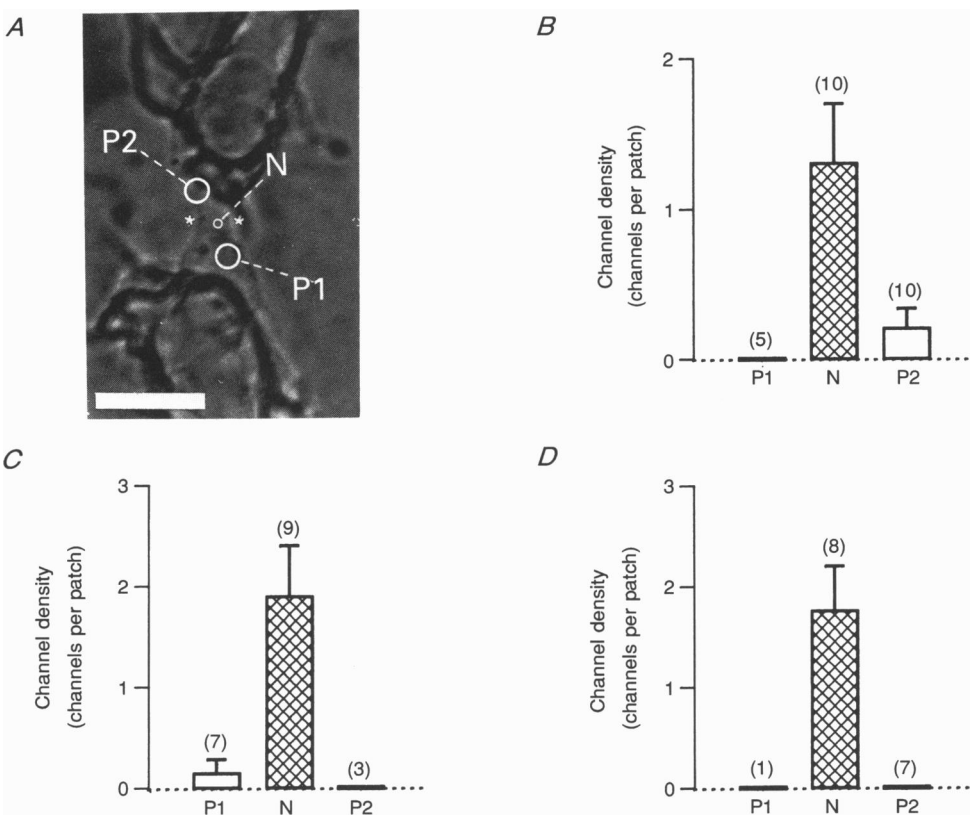

Figure 7. Distribution of axonal K^+_{Na} channels
A, light microscopic view of a demyelinated axon from which several (in total 27) patches were obtained in the nodal region (N, 'central bulge' marked by asterisks) and at two paranodal sites on either side of the node (P1 and P2). Areas marked by circles denote these regions. The picture was taken after the last patch. Scale bar 50 μm. *B*, average number of K^+_{Na} channels per patch at N, P1 and P2 for the axon shown in *A*. Number of patches indictated in parentheses above each bar; two additional patches formed in the region between N and P1, P2 did not contain any K^+_{Na} channels. Bath: 105 mM K^+_i containing 100 mM Na^+; pipette: 105 mM K^+_o. Membrane potential −90 mV. The number of K^+_{Na} channels in the patch was estimated from the maximum number of superimposed openings in the axon-attached and, subsequently, in the inside-out configuration. The channel activity in both recording modes was similar, presumably because Na^+ ions had diffused into the nodal region through the cut-open ends of the nerve fibres (Koppenhöfer & Vogel, 1969; Palti, Gold & Stämpfli, 1979). Pipette resistances were around 20 MΩ in this set of experiments. *C* and *D*, cartography of two other axons. Pipette resistances were about 12 and 15 MΩ, respectively.

(Fig. 6*A*). Accordingly, the mean current during a long recording was reduced, whereas the single-channel current remained unaffected (Fig. 6*D*). This indicates that the Ba^{2+} block occurred on a much slower time scale than the block by TEA^+. The inhibition of the K^+_{Na} channel by Ba^{2+} ions was strongly potential dependent, being more pronounced at negative than at positive transmembrane voltages (Fig. 6*D*). Half-maximal inhibition was observed with a concentration of 0·7 mM at −90 mV (Fig. 6*E*).

The inhibition of the axonal K^+_{Na} channel by external Cs^+ ions was distinct from both TEA^+ and Ba^{2+} block. Cs^+ (10 mM) at −90 mV almost completely abolished single-channel events (Fig. 6*A*). As with the block by TEA^+, single-channel current and mean current during a long recording were reduced to a similar extent, suggesting a fast inhibition mechanism (Fig. 6*F*). Like the block by Ba^{2+}, Cs^+ acted in a strongly potential-dependent manner, being more effective at negative than at positive transmembrane voltages (Fig. 6*F*). Half-maximal inhibition was observed with a concentration of 1·1 mM at −90 mV (Fig. 6*G*). The Hill coefficient was greater than 1, suggesting that more than one Cs^+ ion binds to one K^+_{Na} channel.

The 'fast blockers' TEA^+ and Cs^+ seemed to reduce the amplitude of the subconductance states and the main conductance state by a similar factor. In the presence of each of the blockers, subconductance states occurred with roughly the same frequency as compared with control conditions (see Wang *et al.* 1991 for Ba^{2+} block).

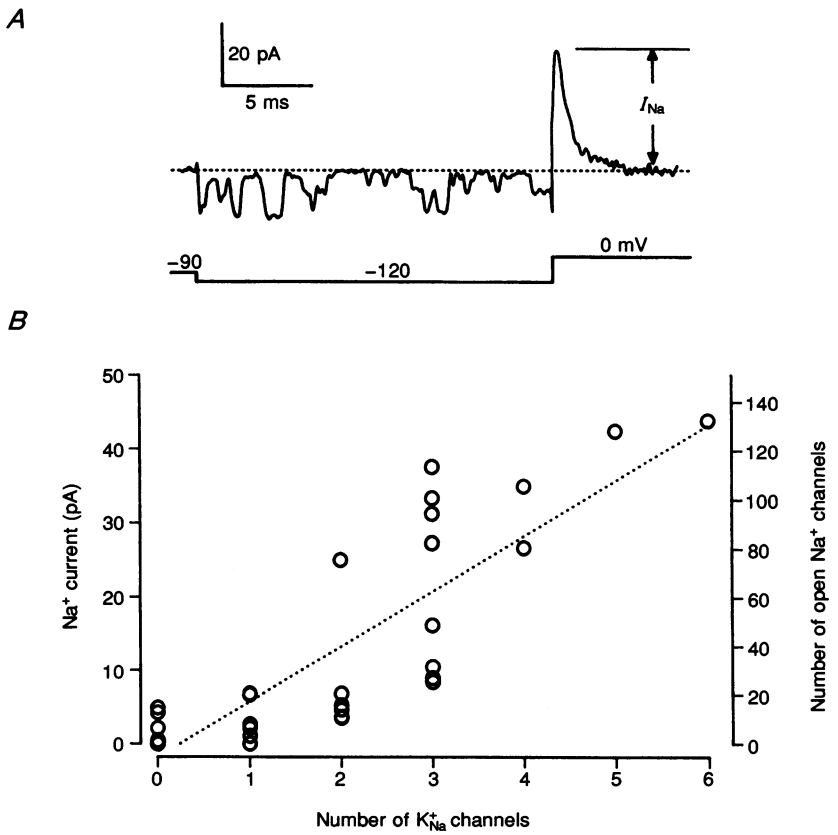

Figure 8. Co-localization of Na^+ channels and K^+_{Na} channels
A, Na^+ outward current evoked by a test pulse to 0 mV preceded by a 20 ms prepulse to −120 mV, single trace corrected for leakage and capacitive currents. Inside-out patch. Bath: 105 mM K^+_i containing 100 mM Na^+; pipette: 105 mM K^+_o (TTX free, containing 3 mM TEA^+ to block the delayed rectifier K^+ channels). During the test pulse, the driving force on K^+ and Cl^- ions was negligible, and the Na^+ current could thus be studied in isolation. Note K^+_{Na} channel events during the prepulse. The maximum number of superimposed openings of K^+_{Na} channels was five in this experiment. *B*, amplitude of Na^+ peak current plotted as a function of the number of K^+_{Na} channels. For the measurement of peak Na^+ currents, averages of ten single traces were used. The right ordinate indicates the corresponding number of Na^+ channels open at the peak, calculated using a single-channel current of 0·33 pA (measured under similar conditions as in *A*, filter frequency 2 kHz, data not shown, 4 patches). Pipette resistances ranged from 5 to 13 MΩ. In total 37 inside-out patches were obtained from 10 axons at nodal and paranodal locations. The dotted line is drawn according to linear regression analysis.

Distribution of the K^+_{Na} channel along the axon

The distribution of K^+_{Na} channels in the axonal membrane was characterized by obtaining several membrane patches from the same axon at different locations. Figure 7*A* shows a demyelinated axon from which twenty-seven membrane patches in total had been isolated, from the nodal region as well as the paranodal regions on either side. A bar diagram illustrating the distribution of K^+_{Na} channels in this axon is shown in Fig. 7*B*. The average channel density found in the nodal region was 1·3 channels per patch, whereas the channel density at the paranodal sites was much lower: 0 and 0·2 channels per patch, respectively. Similar results were obtained for two other axons from which nineteen and sixteen membrane patches could be isolated (Fig. 7*C* and *D*). These results suggest that the density of axonal K^+_{Na} channels is highest at the node of Ranvier, and that there is a steep gradient towards the paranodal region.

The classic example of an ionic channel segregated to the nodal region of an axon is the voltage-dependent Na^+ channel (Hille, 1992). We investigated therefore if and to what degree K^+_{Na} channels and Na^+ channels are co-localized within the same axonal membrane patch. In several patches obtained from nodal and paranodal sites, the size of Na^+ current elicited by a voltage pulse (Fig. 8*A*) and the number of K^+_{Na} channels were determined (see figure legend and Methods for details). The results are illustrated as a scatter plot (Fig. 8*B*). The number of voltage-dependent Na^+ channels and the number of K^+_{Na} channels per patch showed a significant correlation (linear regression, $r = 0{\cdot}86$, $P < 0{\cdot}001$). These results provide further strong evidence that K^+_{Na} channels are spatially restricted to the nodal region of the axolemma where they are co-localized with voltage-dependent Na^+ channels.

DISCUSSION

In the present study, we have identified a K^+-selective channel in vertebrate axons which is activated by internal Na^+ ions. It is relatively insensitive to external TEA^+ but is blocked by Ba^{2+} and Cs^+ ions. K^+_{Na} channels are segregated in the nodal region of myelinated nerve fibres and are co-localized with voltage-dependent Na^+ channels. Considering all functional properties, the axonal K^+_{Na} channel is clearly distinct from the other types of K^+ channels identified until now in myelinated nerve fibres: showing only slight potential dependence and weak TEA sensitivity, it differs from the delayed rectifier K^+ channels (Jonas *et al.* 1989; Safronov, Kampe & Vogel, 1993). Unlike the axonal Ca^{2+}-dependent K^+ channel (Jonas *et al.* 1991), the K^+_{Na} channel does not require internal Ca^{2+} ions to be activated. In contrast to the axonal ATP-sensitive K^+ channel (Jonas *et al.* 1991), it is not inhibited by internal adenosine-5′-triphosphate (ATP, 1 mM, data not shown). With respect to its pharmacological properties and the weak potential dependence, the K^+_{Na} channel shows some similarities to the flickering K^+ channel described in myelinated nerve (Koh *et al.* 1992). The flickering channel, however, can be distinguished from the K^+_{Na} channel by its faster gating kinetics and its lower single-channel conductance.

Comparison with K^+_{Na} channels in other cell types

K^+ channels activated by internal Na^+ ions were first described in heart cells (Kameyama *et al.* 1984). From measurements of macroscopic whole-cell currents, it was inferred that K^+_{Na} channels might also be present in nerve cells (Bader *et al.* 1985); more recently, they have been demonstrated directly on the single-channel level in the somata of brainstem, sensory ganglia and olfactory bulb neurones (Dryer *et al.* 1989; Haimann *et al.* 1990; Egan *et al.* 1992; Dryer, 1993). So far, K^+_{Na} channels have only been reported in excitable cells. Compared with other K^+ channels which are modulated by cytoplasmic factors, such as Ca^{2+}-activated and ATP-sensitive channels, they seem to be less ubiquitously distributed among several cell types, suggesting a more specific functional role.

The functional properties of axonal K^+_{Na} channels are similar to those of K^+_{Na} channels in heart and neuronal somata in many respects. The half-maximal activating concentration for internal Na^+ ions of the axonal channel is in reasonable agreement with the values of 66 mM (Kameyama *et al.* 1984) and 27 mM (Haimann *et al.* 1990) reported for heart and sensory ganglia, respectively. In all cases, the Hill coefficient ranged between 2 and 3, suggesting the co-operative binding of possibly three Na^+ ions to one channel molecule. This co-operative binding may be of functional relevance, making the channel sensitive to very small changes of $[Na^+]_i$ (see below). Other common functional properties of K^+_{Na} channels in different cell types are the weak potential dependence of open probability (Kameyama *et al.* 1984; Haimann *et al.* 1990; however, also see Dale, 1993) and the frequent occurrence of various subconductance levels (Haimann *et al.* 1990; Wang *et al.* 1991). The present study provides a quantitative pharmacological analysis of the axonal K^+_{Na} channel which was not available before. Weak sensitivity to external TEA^+ and block by Ba^{2+} ions, however, have been described previously (Dryer *et al.* 1989; Wang *et al.* 1991).

The single-channel conductance of the axonal K^+_{Na} channel (88 pS; 15 °C and 105 mM $[K^+]_o$) is considerably smaller than that reported previously for cardiac myocytes (220 pS; 30–35 °C and 150 mM $[K^+]_o$; Kameyama *et al.* 1984) and different types of neurones (100 pS, Dryer *et al.* 1989; 174 pS, Haimann *et al.* 1990; 172 pS, Egan *et al.* 1992; 22 °C and 150 mM $[K^+]_o$ in all cases). This difference can be attributed, at least partly, to the lower temperature and the lower external K^+ concentration in the present study. Alternatively, it is possible that

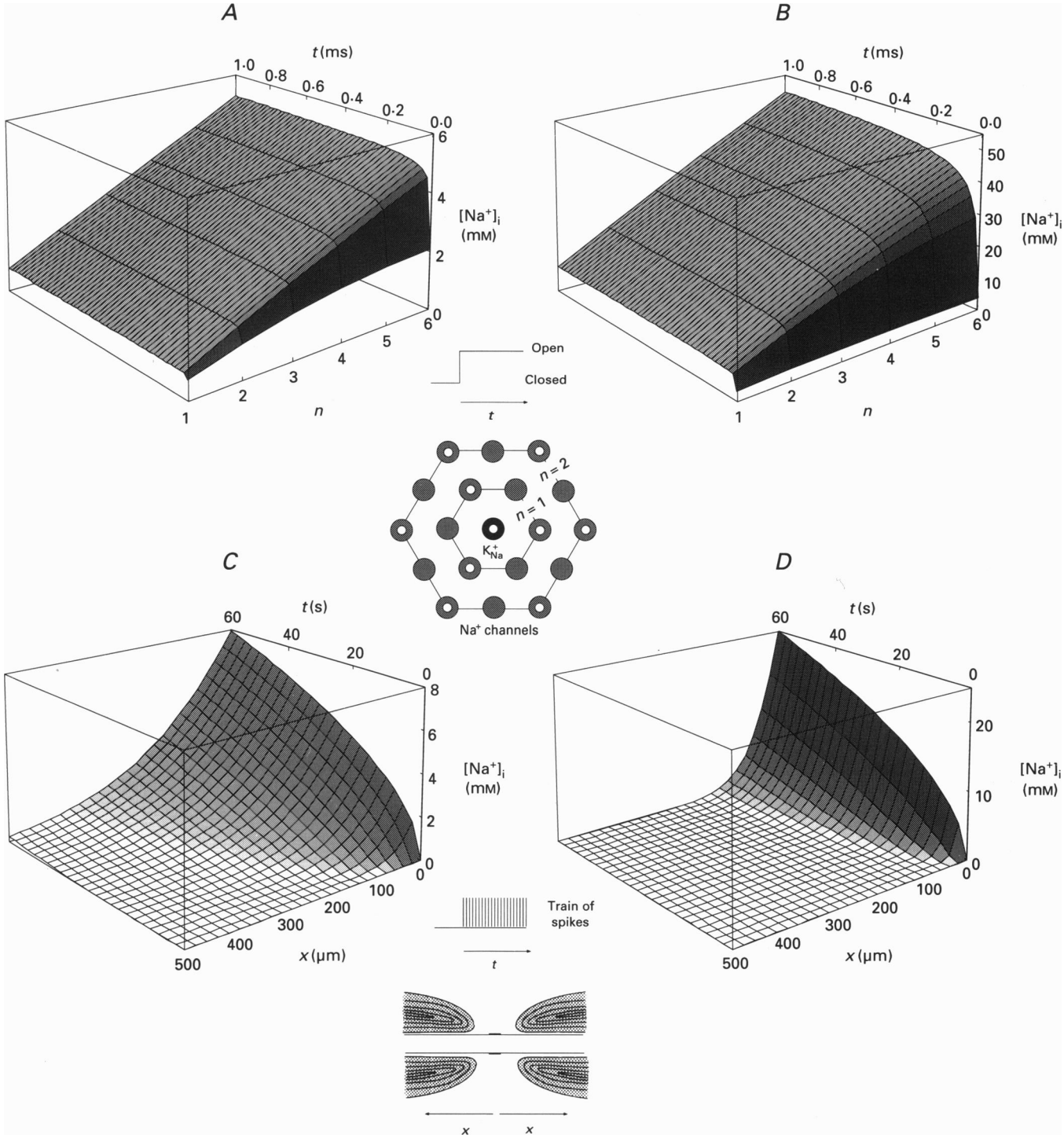

Figure 9. Theoretical calculation of diffusion and accumulation of Na^+ ions
A and *B*, simulation of increase of $[Na^+]_i$ in an assembly of one K^+_{Na} channel surrounded by up to six layers of Na^+ channels (see schematic drawing below). $[Na^+]_i$ is plotted against the number of hexagonal rings of surrounding Na^+ channels, n, and time after simultaneous opening of half of the channels, t. Calculation according to eqn (2), $\Phi_{channel} = 1{\cdot}04 \times 10^{-17}$ M s^{-1}, distance between channels 10 nm. *C* and *D*, simulation of increase of $[Na^+]_i$ in an axon during a train of action potentials (see scheme below). $[Na^+]_i$ is plotted against the distance from the node, x (1–500 μm), and time after beginning of the train of spikes, t (1 μs to 60 s). Calculation according to eqn (4). Axon radius 5 μm, nodal gap 1 μm, Na^+ influx at the node $\Phi_{train} = 3{\cdot}5 \times 10^{-15}$ M s^{-1}. Diffusion coefficient was assumed as $D_i = 0{\cdot}6 \times 10^{-5}$ cm^2 s^{-1} (for *A* and *C*) and $D_{0\cdot1} = 0{\cdot}6 \times 10^{-6}$ cm^2 s^{-1} (for *B* and *D*). For further details see Methods and Discussion.

different K^+_{Na} channel subtypes with different elementary conductances are expressed in various types of excitable cells.

Possible function of K^+_{Na} channels at the node of Ranvier

The functional role of K^+_{Na} channels in heart and neurones has been somewhat controversial (e.g. Dryer, 1991). The first question that arises is whether the axoplasmic Na^+ concentration at rest could be high enough to activate a significant fraction of K^+_{Na} channels. The intracellular Na^+ concentration in myelinated axons has been determined as 22 mM using electron X-ray probe analysis (Lopachin, Castiglia & Saubermann, 1992). If $[Na^+]_i$ in the intact axon is this high, a fraction of K^+_{Na} channels might be active at rest, and the molecular basis of 'leakage' current and resting potential of axons might be more complex than previously anticipated. Depending on the concentration of various cytoplasmic factors, like Na^+, ATP and Ca^{2+}, several different channels (this paper; Jonas *et al.* 1991; Koh *et al.* 1992) could contribute to the resting potential of myelinated nerve fibres.

In addition to the possible contribution of axonal K^+_{Na} channels to the resting potential under physiological conditions, it is conceivable that they may play a, possibly more important, role under pathophysiological conditions, like hypoxia of peripheral nerve. In this situation, a failure of the Na^+–K^+ pump occurs, and $[Na^+]_i$ can rise severalfold (Galvan *et al.* 1984). A putative functional role of K^+_{Na} channels would then be to prevent excessive depolarization and thereby to maintain the membrane potential of the myelinated nerve fibre at its resting value.

Is the Na^+ entry during a single action potential sufficient to activate K^+_{Na} channels? Dryer (1991) demonstrated that the influx through a single Na^+ channel and the resulting local increase of Na^+ concentration is *not* sufficient to activate a neighbouring K^+_{Na} channel even if both are closely attached to each other. The present paper provides experimental evidence to show that K^+_{Na} channels and Na^+ channels are co-localized microscopically within the same axonal membrane patch. Moreover, the scatter plot shown in Fig. 8 suggests that each K^+_{Na} channel could be surrounded by several Na^+ channels. Figure 9*A* and *B* illustrates the results of a theoretical calculation of the increase of $[Na^+]_i$ in an assembly of one K^+_{Na} channel surrounded by several hexagonal layers of Na^+ channels (see Methods, and Dryer, 1991), providing the highest possible packing density (10 nm distance between channel centres). $[Na^+]_i$ at the centre of the assembly was plotted *versus* the number of Na^+ channel layers and time after simultaneous opening of half of the channels. For six hexagonal layers, corresponding to 126 Na^+ channels, $[Na^+]_i$ increases by 4 mM assuming a diffusion coefficient, D_1, of $0{\cdot}6 \times 10^{-5}$ cm^2 s^{-1}, the value generally accepted for diffusion of Na^+ ions in cytoplasm (Kushmerick & Podolsky, 1969). $[Na^+]_i$ rises to even higher values when diffusion barriers are assumed ($D_{0{\cdot}1} = 0{\cdot}6 \times 10^{-6}$ cm^2 s^{-1}). Notably, the rise in Na^+ concentration occurs very rapidly, within less than 1 ms. This suggests that, depending on the exact packing density and geometry of Na^+ channels, the rise in Na^+ concentration during a single action potential might be sufficient to activate K^+_{Na} channels and to thereby accelerate spike repolarization at the node of Ranvier. However, the fact that TEA-resistant, time-dependent outward currents are not obvious in macroscopic voltage clamp experiments (e.g. Hille, 1967) implies that the current through K^+_{Na} channels is probably small and masked by other current components, e.g. maintained Na^+ inward currents (Dubois & Bergman, 1975).

Is the Na^+ influx during a high-frequency train of action potentials sufficient to activate K^+_{Na} channels? The Na^+ influx during a spike train could result in a long-lasting rise of $[Na^+]_i$ in the whole cytoplasmic compartment, as opposed to the transient and local increase of $[Na^+]_i$ for the single spike described above. Whereas this effect may be negligible in somata of neurones with a low density of Na^+ channels and a small surface-to-volume ratio (Dryer *et al.* 1989), it might play a much more important role in small cell processes, like dendrites and axons. We calculated the increase of $[Na^+]_i$ during a sustained train of action potentials (250 Hz) for a cylinder resembling the axonal geometry of a typical A fibre (5 μm radius). In Fig. 9*C* and *D*, $[Na^+]_i$ was plotted *versus* the distance from the node and time after the beginning of the train of spikes. After 60 s, $[Na^+]_i$ in the nodal region increases by almost 10 mM assuming almost free diffusion (D_1). $[Na^+]_i$ rises to even higher values when diffusion barriers are assumed ($D_{0{\cdot}1}$), or in thinner fibres (not illustrated). In accordance with these findings, Bergman (1970) observed a shift of the reversal potential of Na^+ currents by 24–28 mV after a train of action potentials in myelinated nerve fibres, corresponding to an increase of $[Na^+]_i$ by a factor of almost three. The theoretical considerations and the experimental observations together imply that the rise of axoplasmic $[Na^+]_i$ in the nodal region during tetanic stimulation could be sufficient to activate K^+_{Na} channels. This suggests that K^+_{Na} channels could contribute to post-tetanic after-hyperpolarizations in axons. It is generally thought that post-tetanic after-hyperpolarizations in nerve cells are at least partly caused by the activity of the electrogenic Na^+–K^+ pump (e.g. Thomas, 1972). It has been a matter of controversy, however, as to whether post-tetanic after-hyperpolarizations in peripheral nerve are suppressed by metabolic inhibitors (Meves, 1961; Hurlbut, 1965; Schoepfle, 1976). Axonal K^+_{Na} channels might provide a basis for a re-interpretation of these observations.

In conclusion, two factors may facilitate the activation of K^+_{Na} channels in myelinated nerve fibres: the co-localization of voltage-dependent Na^+ channels and K^+_{Na} channels, i.e. of donor and acceptor channels, and the high Na^+ channel density at the node as opposed to the small intracellular volume of the axonal compartment. Although

axonal K^+_{Na} channels might be open at rest, it seems likely that their activation is promoted further by a single action potential or by a high-frequency train of action potentials. What the most important functional role of K^+_{Na} channels in intact axons is, however, remains to be elucidated.

REFERENCES

BADER, C. R., BERNHEIM, L. & BERTRAND, D. (1985). Sodium-activated potassium current in cultured avian neurones. *Nature* **317**, 540–542.

BERGMAN, C. (1970). Increase of sodium concentration near the inner surface of the nodal membrane. *Pflügers Archiv* **317**, 287–302.

BERTHOLD, C. H. (1978). Morphology of normal peripheral axons. In *Physiology and Pathobiology of Axons*, ed. WAXMAN, S. G., pp. 3–63. Raven Press, New York.

BERTHOLD, C. H. & RYDMARK, M. (1983). Anatomy of the paranode–node–paranode region in the cat. *Experientia* **39**, 964–976.

BÜHRLE, C. P. & SONNHOF, U. (1983). Intracellular ion activities and equilibrium potentials in motoneurones and glia cells of the frog spinal cord. *Pflügers Archiv* **396**, 144–153.

CRANK, J. (1975). *The Mathematics of Diffusion*. Clarendon Press, Oxford.

DALE, N. (1993). A large, sustained Na^+- and voltage-dependent K^+ current in spinal neurons of the frog embryo. *Journal of Physiology* **462**, 349–372.

DRYER, S. E. (1991). Na^+-activated K^+ channels and voltage-evoked ionic currents in brain stem and parasympathetic neurones of the chick. *Journal of Physiology* **435**, 513–532.

DRYER, S. E. (1993). Properties of single Na^+-activated K^+ channels in cultured central neurons of the chick embryo. *Neuroscience Letters* **149**, 133–136.

DRYER, S. E., FUJII, J. T. & MARTIN, A. R. (1989). A Na^+-activated K^+ current in cultured brain stem neurones from chicks. *Journal of Physiology* **410**, 283–296.

DUBOIS, J. M. & BERGMAN, C. (1975). Late sodium current in the node of Ranvier. *Pflügers Archiv* **357**, 145–148.

EGAN, T. M., DAGAN, D., KUPPER, J. & LEVITAN, I. B. (1992). Properties and rundown of sodium-activated potassium channels in rat olfactory bulb neurons. *Journal of Neuroscience* **12**, 1964–1976.

FRANKENHAEUSER, B. & HUXLEY, A. F. (1964). The action potential in the myelinated nerve fibre of *Xenopus laevis* as computed on the basis of voltage clamp data. *Journal of Physiology* **171**, 302–315.

GALVAN, M., DÖRGE, A., BECK, F. & RICK, R. (1984). Intracellular electrolyte concentrations in rat sympathetic neurones measured with an electron microprobe. *Pflügers Archiv* **400**, 274–279.

HAIMANN, C., BERNHEIM, L., BERTRAND, D. & BADER, C. R. (1990). Potassium current activated by intracellular sodium in quail trigeminal ganglion neurons. *Journal of General Physiology* **95**, 961–979.

HAMILL, O. P., MARTY, A., NEHER, E., SAKMANN, B. & SIGWORTH, F. J. (1981). Improved patch-clamp techniques for high-resolution current recording from cells and cell-free membrane patches. *Pflügers Archiv* **391**, 85–100.

HILLE, B. (1967). The selective inhibition of delayed potassium currents in nerve by tetraethylammonium ion. *Journal of General Physiology* **50**, 1287–1302.

HILLE, B. (1992). *Ionic Channels of Excitable Membranes*. Sinauer, Sunderland, MA, USA.

HURLBUT, W. P. (1965). Salicylate: effects on ion transport and afterpotentials in frog sciatic nerve. *American Journal of Physiology* **209**, 1295–1303.

JONAS, P., BRÄU, M. E., HERMSTEINER, M. & VOGEL, W. (1989). Single-channel recording in myelinated nerve fibers reveals one type of Na channel but different K channels. *Proceedings of the National Academy of Sciences of the USA* **86**, 7238–7242.

JONAS, P., KOH, D.-S., KAMPE, K., HERMSTEINER, M. & VOGEL, W. (1991). ATP-sensitive and Ca-activated K channels in vertebrate axons: novel links between metabolism and excitability. *Pflügers Archiv* **418**, 68–73.

KAMEYAMA, M., KAKEI, M., SATO, R., SHIBASAKI, T., MATSUDA, H. & IRISAWA, H. (1984). Intracellular Na^+ activates a K^+ channel in mammalian cardiac cells. *Nature* **309**, 354–356.

KOH, D.-S., JONAS, P., BRÄU, M. E. & VOGEL, W. (1992). A TEA-insensitive flickering potassium channel active around the resting potential in myelinated nerve. *Journal of Membrane Biology* **130**, 149–162.

KOH, D.-S. & VOGEL, W. (1992). Na-activated K channels localized in the nodal area of myelinated nerve. *Pflügers Archiv* **420**, R27.

KOPPENHÖFER, E. & VOGEL, W. (1969). Wirkung von Tetrodotoxin und Tetraäthylammoniumchlorid an der Innenseite der Schnürringsmembran von *Xenopus laevis*. *Pflügers Archiv* **313**, 361–380.

KUSHMERICK, M. J. & PODOLSKI, R. J. (1969). Ionic mobility in muscle cells. *Science* **166**, 1297–1298.

LOPACHIN, R. M., CASTIGLIA, C. M. & SAUBERMANN, A. J. (1992). Perturbation of axonal elemental composition and water content: Implication for neurotoxic mechanisms. *NeuroToxicology* **13**, 123–138.

MEVES, H. (1961). Die Nachpotentiale isolierter markhaltiger Nervenfasern des Frosches bei tetanischer Reizung. *Pflügers Archiv* **272**, 336–359.

PALTI, Y., GOLD, R. & STÄMPFLI, R. (1979). Diffusion of ions in myelinated nerve fibers. *Biophysical Journal* **25**, 17–31.

PATLAK, J. B. (1988). Sodium channel subconductance levels measured with a new variance–mean analysis. *Journal of General Physiology* **92**, 413–430.

RANSCHT, B., CLAPSHAW, P. A., PRICE, J., NOBLE, M. & SEIFERT, W. (1982). Development of oligodendrocytes and Schwann cells studied with a monoclonal antibody against galactocerebroside. *Proceedings of the National Academy of Sciences of the USA* **79**, 2709–2713.

SAFRONOV, B. V., KAMPE, K. & VOGEL, W. (1993). Single voltage-dependent potassium channels in rat peripheral nerve membrane. *Journal of Physiology* **460**, 675–691.

SCHOEPFLE, G. M. (1976). Tetanic hyperpolarization of single medullated nerve fibers in sodium and lithium. *American Journal of Physiology* **231**, 1033–1038.

STÄMPFLI, R. & HILLE, B. (1976). Electrophysiology of the peripheral myelinated nerve. In *Frog Neurobiology*, ed. LLINÁS, R. & PRECHT, W., pp. 3–32. Springer-Verlag, Berlin.

THOMAS, R. C. (1972). Electrogenic sodium pump in nerve and muscle cells. *Physiological Reviews* **52**, 563–594.

WANG, Z., KIMITSUKI, T. & NOMA, A. (1991). Conductance properties of the Na^+-activated K^+ channel in guinea-pig ventricular cells. *Journal of Physiology* **433**, 241–257.

YELLEN, G. (1982). Single Ca^{2+}-activated nonselective cation channels in neuroblastoma. *Nature* **296**, 357–359.

Acknowledgements

We thank Drs M. Häusser and A. Villarroel for critically reading the manuscript, Dr E. v. Kitzing and A. Roth for many helpful discussions. This work was supported by the Deutsche Forschungsgemeinschaft (Vo 188/13–2).

Received 2 September 1993; accepted 13 January 1994.